Identification of Plant Sphingolipid Desaturases Using Chromatography and Mass Spectrometry

Dayong Sun[1,*], Byron E. Froman[2], Robert G. Orth[1], Susan A. MacIsaac[1], Thomas Larosa[1], Fenggao Dong[1], and **Henry E. Valentin[2]**

[1]Monsanto Company, 800 N Lindbergh Blvd, St. Louis, MO 63167 and [2]Monsanto Company, Calgene Campus, 1920 Fifth Street, Davis, CA 95616

Abstract

This manuscript describes an efficient analytical assay combining high-performance liquid chromatography with UV detection (HPLC–UV), liquid chromatography coupled with tandem mass spectrometry (LC–MS–MS), and gas chromatography with mass spectrometry (GC–MS) for the characterization and C=C bond localization on the long chain base of sphingolipids in yeast extracts in order to identify the plant sphingolipid desaturases activity. Samples of wild type control and transgenic yeast expressing putative sphingolipid desaturases were hydrolyzed into long chain bases. Mono-unsaturated long chain base, dehydrophytosphingosine (t18:1), in transgenic yeast as a result of the function of plant sphingolipid desaturase was detected with cis, trans-isomers resolution by reverse phase HPLC–UV as DNP (2,4-dinitrophenyl) derivatives along with saturated phytosphingosine (t18:0). The molecular structure of phytosphingosine was confirmed by negative-ion LC–MS–MS, which also served as a rapid tool for screening the plant spingolipid desaturase activity with 2-min run time under multiple-reaction monitoring (MRM) mode. The C=C bond location of dehydrophytosphingosine was further identified by GC–MS after being converted into picolinyl derivatives. This assay combines multiple chromatographic and mass spectrometric techniques with gentle chemical procedures to provide capacities for rapid determination of the plant sphingolipid desaturase activity as well as identification of their active sites in the backbone of the sphingolipid species in yeast.

Introduction

Sphingolipids are major membrane lipids playing essential physiological roles in signal transmission, cell growth mediation, cell differentiation, cell recognition, and cell death (1–4). They are commonly believed to protect the cell surface against harmful environmental factors by forming a mechanically stable and chemically resistant outer barrier of the plasma membrane lipid bi-layer. The characteristic backbone or defining structural unit of various sphingolipids are long-chain bases (LCB), which are the aliphatic amines of different chain length and degree of unsaturation, containing two or three hydroxyl groups (Figure 1). Depending on the hydrophilic head groups, there are three main types of sphingolipids: ceramides, sphingomyelins, and glycosphingolipids. Recently, research on the structures and functions of complex sphingolipids, LCBs and their degradation products has been rapidly expanding (5–16). Emerging areas, such as "sphingolipidomics" and sphingolipid-MALDI-TOFMS imaging have become very valuable tools to improve the understanding of the importance of these bioactive lipids in various biological systems, particularly their catabolism as secondary messengers in plants and fungi (17–20).

Our understanding of the molecular basis of sphingolipid biosynthesis is still very limited, and the first plant gene encoding a sphingolipid desaturase has been cloned only in recent years (21). In order to identify unknown sphingolipid desaturases, an analytical assay has to satisfy two aspects. First is the confirmation of sphingolipid desaturase activity—detection and molecular structure identifation of new unsaturated sphingolipid species that have been formed as a result of the function of plant sphingolipid desaturases. Second is to locate the C=C bond position in the unsaturated sphingolipid species to identify the desaturases active sites in the backbone of the sphingolipid species. There have previously been a few reports on this purpose by either using high-performance liquid chromatography (HPLC)–OPA derivatization or gas chromatography with mass spectrometry (GC–MS)-nicotinate derivatization (22–30). These

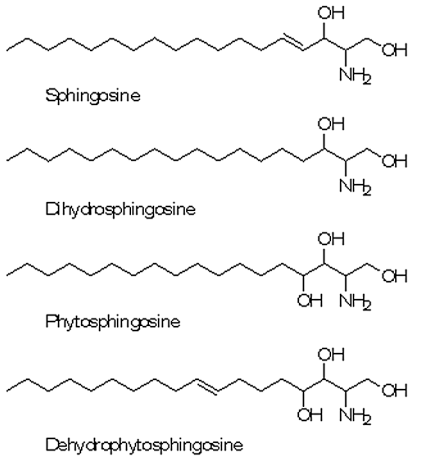

Figure 1. Molecular structures of long chain bases (LCB): sphingosine (Δ4-d18:1), dihydrosphingosine (d18:0), phytosphingosine (t18:0), and dehydrophytosphingosine (Δ8-t18:1), where "d" and "t" represent the numbers of hydroxyl groups, "18:0" or "18:1" represent the lengths and degree of unsaturation of the fatty aliphatic amines chain.

* Author to whom correspondence should be sent: Dayong Sun, Mail Zone: S3C, Monsanto Company, 800 N. Lindbergh Blvd. St. Louis, MO 63167, e-mail dsun@monsanto.com.

methods are effective, but they either only detect the desaturase activity and can't localize the C=C position or lack efficiency due to the use of tedious multiple-step thin-layer chromatography purification. Efficiency is also frequently hampered by complicated wet chemistry reactions using highly reactive and hazardous chemicals and the need of fatty acid nicotinate derivatives as the final products to locate the C=C position by GC–MS. The identification of the nicotinate derivatives is compromised by a lack of standard spectra for comparation. We report herein a comprehensive set of analytical solutions combining HPLC, liquid chromatography coupled with tandem mass spectrometry (LC–MS–MS), and GC–MS for sphingolipid desaturase identification. Reverse phase HPLC–UV and high throughput LC–MS–MS are used to readily determine the plant sphingolipid desaturases activities in transgenic yeast by detecting and identifying the formation of mono-unsaturated LCBs after sphingolipid hydrolysis and derivatization. The LCB derivatives were then converted into fatty acid picolinyl derivatives for GC–MS to locate the C=C bond positions. Compared to previous approaches, this assay uses gentle chemical reactions, new analytical means, and fatty acid picolinyl derivatives as final products to locate the C=C position. This has the advantage of improved identification confidence with well-established standard spectra available. This method is efficient, convenient, and has the flexibility to be used to either confirm the "tentative" sphingolipid desaturase activity by HPLC and LC–MS or as a high throughput screening tool to select active sphingolipid desaturase for a large set of samples by LC–MS under multiple-reaction monitoring (MRM). In addition, it can be used for a complete identification of "unknown" sphingolipid desaturase by combining HPLC, LC–MS, and GC–MS.

Materials and Methods

Cloning of *Primula* Δ8 sphingolipid desaturase genes

Cloning of the *Primula nivalis* Δ8 sphingolipid desaturase, *PnSLD1*, was achieved by PCR amplification of a partial internal genomic DNA fragment using degenerate oligonucleotides followed by determining the flanking sequence by inverse PCR (IPCR). Total genomic DNA was isolated from young leaves of *Primula nivalis* (Fritz Creek Gardens, Homer, AK) using the DNeasy Plant Mini Kit (Qiagen, Valencia, CA) following the manufacturer's recommendations. An internal 552bp fragment was PCR amplified using the degenerate oligonuclotide primers BO-1 (5'-ATMAGYATYGGTTGGTGGAARTGG-3') and BO-2 (5'-AATCCACCRTGRAACCARTCCAT-3') (30). IPCR was utilized to obtain the genomic 5'- and 3'-flanking sequences using the primers Pn1109-2F1 (5'-CGGATAAAACGACCAATGCT-3') and Pn1109-2R1 (5'-AGGTGTGTTTTGGGTTTGGT-3') with the Expand Long Template PCR System (Roche Applied Science, Indianapolis, IN) (31). Thermal cycle conditions consisted of an initial incubation at 94°C for 2 min; 94°C for 20 s, 52°C for 30 s, and 68°C for 8 min (10 cycles); followed by 94°C for 30 s, 52°C for 30 s and 68°C for 8 min (25 cycles) plus 10 s per cycle. After cycling was complete, a further incubation at 68°C for 7 min was performed. A composite sequence containing the internal core and flanking regions revealed on open reading frame (ORF) of 1359 nucleotides encoding a protein consisting of 453 amino acids. The full-length coding region was obtained by PCR amplification employing the primers Pnivales1994F 5'-CAACCACTTGTATCAATCAGCTTACTCAACCT-3' and Pnivales3756R 5'-GCCCCTAGGAAGACAATCAGGATAACA-3', which was subsequently ligated into the yeast expression vector pYES2.1/V5-His-TOPO (Invitrogen, Carlsbad, CA) to give pMON67066. The P. nivalis Δ8 sphingolipid desaturase sequence is available under GenBank Accession # GQ981650".

Cloning of the *Primula auricula* Δ8 sphingolipid desaturase, *PaSLD1*, was achieved by PCR amplification of a partial internal cDNA fragment using degenerate oligonucleotides Primer P1 and Primer P2, followed by rapid amplification of cDNA ends (RACE) using primers GPS1 and GSP2 to determine the 5' and 3' sequences of the transcript. Total RNA was isolated from young leaves of *Pimula auricula* (Fritz Creek Gardens, Homer, AK) using the RNAeasy kit (Qiagen). PolyA$^+$ RNA was purified from total RNA using oligo(dT) cellulose (32) and was reverse transcribed using the Reverse Transcription System from Promega (Madison, WI). An internal fragment was PCR amplified using the degenerate primers, Primer Pn1 (5'-GGITGGHTIGGICAYGAYKYIKSICA-3') and Primer Pn2 (5'-GGRAAIAGRTGRTGYTCDATYTG-3') and sequenced. Briefly, the reaction mix was 50 µL containing 5–10 µL of first-strand cDNA, 0.18 mM dNTP, 1.8 mM $MgCl_2$ with 25 pmol of Primer P1 and Primer P2, and 1.25 units of Taq DNA polymerase. Thermal cycle conditions consisted of an incubation at 94°C for 1 min, 45°C for 1 min, and 72°C for 2 min (34 cycles); followed by 72°C for 7 min. The RT-PCR procedure generated a 660bp fragment that was gel purified before ligating into the pGEM-T easy vector (Promega, Madison, WI) to determine the sequence. The SMART RACE cDNA Amplification Kit was employed to extend the sequence in the 5' and 3' directions using gene specific primers according to the manufacturer's recommendations (BD-Clontech, Mountain View, CA). Thermal cycle conditions consisted of an incubation at 94°C for 30 s, 68°C for 30 s, and 72°C for 3 min (24 cycles); followed by 72°C for 7 min (GSP T_m < 70°C). The resulting PCR products were ligated into pGEM-T easy vector and the sequence determined. Alignment of the internal region with the 5' and 3' RACE products revealed an ORF of 1356 nucleotides encoding a protein of 452 amino acids. The entire coding region was amplified using BD's Advantage 2 PCR kit. Briefly 2.5 µL of 5'-RACE-Ready cDNA, 0.2 µM of gene specific forward primer Pa1(5'-AAACAATGGGTTCTTTAGGGTTACCCCCAA-3') and reverse primer Pa2 (5'-TCAACCATGTGTGTTAACAGCTTCCCA-3'), 0.2 mM dNTP, and 5 µL of 10X BD Advantage 2 Polymerase Mix was added to a final volume of 50 µL reaction mix. Thermal cycle conditions consisted of an incubation at 94°C for 30s, 68°C for 30 s, and 72°C for 3 min (24 cycles); followed by 72°C for 8 min. The PCR product was ligated into the yeast expression vector pYES2.1/V5-His-TOPO to give pMON95048. The *P. auricula* Δ8 sphingolipid desaturase sequence is available under GenBank Accession # GQ981651.

Yeast transformation and expression

Constructs pMON67066 and pMON95048 were introduced into the host strain *Saccharomyces cerevisiae* INVSc1

(Invitrogen) using the *S.c.* EasyComp Transformation Kit (Invitrogen). Single transgenic colonies were used to inoculate SC minimal media minus uracil with 2% glucose and grown overnight at 30°C according to the manufactures recommendations (Invitrogen). Induction was accomplished by switching the media to SC minimal media minus uracil with 2% galactose and grown for 3 days at 15°C. The yeast cells were collected and lyophilized to dryness prior to analysis.

Chemicals and reagents

LCB standards, sphingosine, dihydrosphingosine, phytospingosine, and chemical reagents 1-fluoro-2, 4-dinitrobenzene, lead(IV) acetate, potassium tert-butoxide, 3-pyridinemethanol were purchased from Sigma Aldrich (St. Louis, MO). Solvents were purchased as HPLC-grade from Sigma Aldrich or Fisher Scientific.

Instrumentation and settings

An Agilent 1100 HPLC system coupled with an autosampler and a UV detector set at 350 nm was used for the analyses. The column used was ODS Hypersil RP-C_{18} (Thermo Electron, 4.6 × 250 mm, 5 µm). The flow rate was set at 1 mL/min. Water (A) and methanol–acetonitrile–isopropanol (10:3:1, v/v/v) (B) served as mobile phase with a linear gradient from 80% B to 100% B over 40 min. The post-run equilibrium time was 10 min, and the injection volume was 10 µL.

For mass spectrometric analysis, an API-3000 MS/MS system (PE SCIEX/Applied BioSystems, Foster City, CA) coupled with a quaternary LC pump (Rheos FLUX Instrument, Reinach, Switzerland) and an HTS PAL autosampler (Leap Technologies, CTC Analytics, Carrboro, NC) was used. An Alltima C_{18} column (4.6 mm × 50 mm, 3 µm) (Alltech, Nicholasville, KY) was used at a flow rate of 1 mL/min. The mobile phase was 100% methanol containing 0.1% formic acid, and the injection volume was 10 µL. MS conditions were: declustering potential –86 eV; focusing potential –330 eV; entrance potential –10 eV; collision energy –26 eV; collision cell exit potential –15 eV; source temperature 350°C; negative-ion mode. MRM ions for LCBs are: t18:0 482.3/162; t18:1 480.3/162.

GC–MS was conducted using an Agilent 6890/5973 GC–MS system under electron ionization mode coupled with an autosampler (Santa Clara, CA). The column used was BPX-90 (SGE, 60 m × 0.25 mm, 0.25-µm film thickness). Splitless inlet temperature: 250°C. Helium gas flow rate: 1 mL/min. Oven temperature program: 110°C increased to 230°C at 10°C/min and kept at 230°C for 25 min. Injection volume: 0.5 µL. Solvent delay time: 10 min.

Hydrolysis of sphingolipid and analytical sample preparation

Approximately 100–400 mg of lyophilized yeast cells were weighed and added to 3–6 mL (1:1 v/v) $Ba(OH)_2$ aqueous solution (concentration of 10% w/v), and 4-dioxane. The hydrolysis was performed at 110°C for 20–24 h. After cooling to room temperature, the LCBs were extracted with $CHCl_3$–dioxane–H_2O (6:1:5, v/v/v). The organic phase was separated and washed with an equal volume of 0.1M KOH and 0.5M KCl solutions and dried under gentle N_2 flow.

LCBs were dissolved in 1 mL methanol containing 5 µL 1-fluoro-2,4-dinitrobenzene. To this solution, 4 mL 2M potassium borate buffer (pH = 10.5) was added drop wise very slowly. The mixture was incubated for 30 min at 60°C. After cooling to room temperature, the LCB dinitrobenzene derivatives were extracted with $CHCl_3$/MeOH/H_2O (8:4:3, v/v/v). The organic phase was collected and dried under N_2 flow. Subsequently, the sample was re-dissolved in methanol and filtered though 0.45-µm syringe filter (25 mm, Nylon) (Xpertek, St. Louis, MO). The solution was kept at –20°C until HPLC or LC–MS–MS analysis.

For GC–MS analysis, methyl esters were generated as follows: The yellowish methanol solution of LCB dinitrobenzene derivatives was dried under N_2 flow, and the brown solid was oxidized using 60 mg lead tetra-acetate in 600 µL benzene at 60°C for 90 min to produce long chain fatty aldehydes. The solution was washed with 1 mL water and 2 mL hexane twice. The organic phase was collected and slowly dried under N_2 flow.

To dissolve the product, 4 mL of dioxane water mixture (1:1) was added. This was followed by the addition of 3.5 mM silver nitrate dissolved in 2 mL of water to convert long chain aldehydes into free fatty acids. Subsequently, 1.6 mmol NaOH in 2 mL of water was added very slowly with stirring at room temperature over a period of 2 h. This was followed by an acid work up to pH = 1 using 6N HCl. Subsequently ether (3 × 6 mL) was used to extract the resultant free fatty acids. The organic phase was collected and dried under N_2.

Methylation was performed in 1 mL freshly made methanol containing 1% sulfuric acid. The solution was heated at 50°C overnight, and fatty acid methyl esters (FAME) were extracted by adding 1 mL water and 2 mL hexane. The solvents were mixed, and the hexane phase was collected after phase separation. The FAME hexane solution was dried under N_2 flow and re-dissolved in 1 mL dry $CHCl_3$. To generate fatty acid picolinyl derivatives, a solution of potassium tert-butoxide in dry THF (100 µL, 1.0 M) was added to 3-hydroxymethylpyridine (200 µL). After homogenization, the FAME $CHCl_3$ solution was added, and the mixture was heated at 45°C for 30 min. After cooling to room temperature, 1 mL aqueous solution of sodium bicarbonate (2.5%) was added, and the organic phase was collected and dried over anhydrous sodium sulfate. $CHCl_3$ was removed under N_2 flow, and 1 mL hexane was added for GC–MS analysis.

Results and Discussions

Two Δ8 sphingolipid desaturase genes were cloned from *Primula nivalis* and *Primula auricula PnSLD1* and *PaSLD1*, respectively. These genes encode potential polypeptides of 453 amino acids and 452 amino acids, respectively. The sequences have high similarity to other front-end desaturases and include the conserved HPGG heme-binding motif found in the *N*-terminal fused cytochrome b5 domain, and three conserved histidine boxes involved in the binding of a di-iron complex (34). The genomic clone obtained from *P. nivalis* does not appear to contain introns when compared with other Δ8 sphingolipid desaturases. The two Δ8 sphingolipid desaturase protein sequences *PnSLD1* and *PaSLD1* are 59% identical. *PnSLD1* is more similar to both *P. vialii* and *P. farinosa* Δ8 sphingolipid desaturase (91%

amino acid identity) (29). *PaSLD1* is more similar to the *Borage* Δ8 sphingolipid desaturase with 70% amino acid identity (33), whereas having a 60% identity with both the *P. vialii* and *P. farinosa* Δ8 sphingolipid desaturases.

For a functional characterization, *PnSLD1* and *PaSLD1* were cloned into pYES2.1/V5-His-TOPO, transformed into yeast, and grown for three days at 15°C. Evidence for sphingolipid desaturase activity can be obtained by the formation of mono-unsaturated sphingolipid species in treated yeast samples compared to wild-type control. Due to the lack of chromo groups, sphingolipids have been hydrolyzed under basic conditions into LCBs and further derivatized to di-nitrobenzene (DNP) derivatives to become UV-detectable. A facile reaction using 2,4-fluoro-dinitrobenzene can effectively replace the LCB amine active proton to yield a stable yellowish compound, which can be directly detected by reversed phase HPLC–UV with baseline separation of saturate and mono-saturate LCB species. Shown in Figure 2 are the HPLC chromatograms of (A) LCB standard mixture; (B) Wild-type control yeast; and two yeast samples expressing putative sphingolipid desaturases expressed from plasmids (C) pMON67066 and (D) pMON95048, respectively. Different from the plasmid control sample, both sphingolipid desaturases expressed yeast samples contained new sphingolipid species at a retention time of 15–17 min, which were further identified as mono-unsaturated dehydrophytosphingosine t18:1 by LC–MS–MS with the appearance of the molecular ions and informative fragmentation patterns as discussed below. Furthermore, clear base-line separation of two isomers of mono-unsaturated dehydrophytosphingosine t18:1 was obtained under this chromatographic condition, and they were identified as cis- and trans-isomers, respectively, due to the fact that they have the same molecular ion and fragmentation pattern under LC–MS–MS conditions, and trans-isomer has slightly decreased polarity (increased retention in reverse phase chromatography). Both sphingolipid desaturases expressed yeast samples showed the appearance of cis- and trans-mono-unsaturated dehydrophytosphingosine but in different relative ratios. The *P. auricula* sphingolipid desaturase expressing yeast sample contained much higher trans-LCB content than the *P. nivalis* sphingolipid expressing sample.

Over the last two decades, the soft ionization and tandem mass spectrometry techniques have been widely used in lipid biochemistry studies (35–42). Negative-ion LC–MS–MS has been utilized to provide further structure information on the mono-unsaturated dehydrophytosphingosine t18:1 species detected earlier in reverse phase-HPLC with the appearance of the molecular ions in Q1 scan mode and informative fragmentation patterns under MS–MS mode. For example, the ESI-MS–MS spectrum of t18:1 LCB-DNP compound is dominated by its molecular ion $(M-H)^-$ at *m/z* 480 amu, which is consistent with theoretical value. Its CID-MS–MS spectrum contains a series of informative fragmentation or re-arrangement ions, including ion $(M-H-DNP-2OH)^-$ at *m/z* 282 amu and ion $(M-H-DNP-2OH-NH_2)^-$ at 253 amu corresponding to long chain amino alcohol and long chain alcohol fragments, and ions at *m/z* 226 corresponding to *N*-hydroxyethyl 2,4-di-nitro-aniline fragment, which are also consistent with its molecular structure. In addition, the high selectivity function of the LC–MS–MS under MRM mode can significantly minimize the matrix interference and reduce the analytical time for high throughput screening application. As shown in Figure 3, saturated and mono-unsaturated LCB-DNP derivatives can be detected by LC–MS–MS with good baseline separation within 1.5 minutes. Thus, this method can be employed as a high throughput screening tool to efficiently select active sphingolipid desaturases from a large sample set for further identification.

Even though reverse phase HPLC–UV and LC–MS–MS can be used to detect and identify the formation of mono-unsaturated

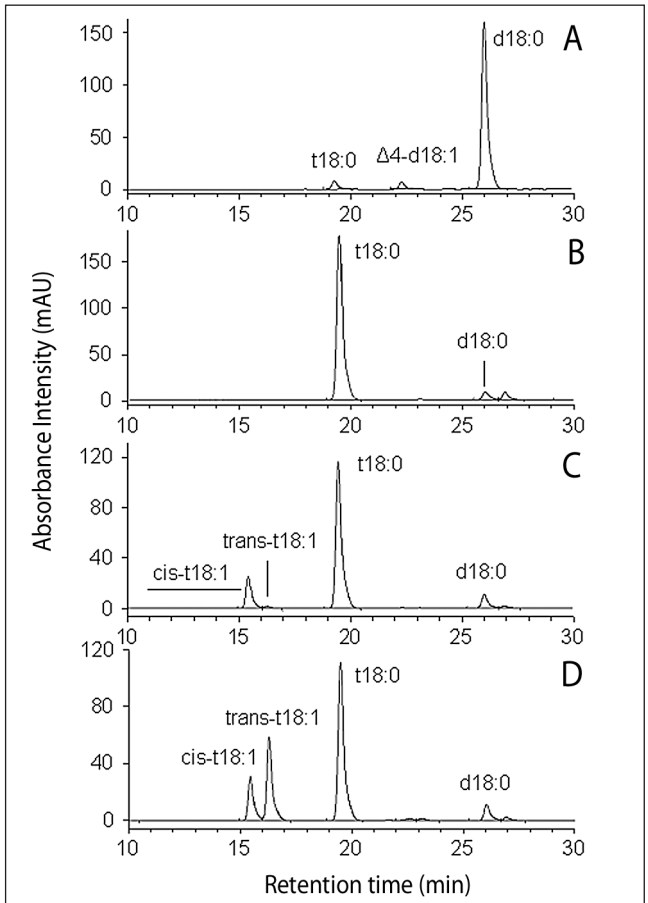

Figure 2. Reverse-phase HPLC–UV (350 nm) chromatograms of the 2,4-di-nitrophenyl derivatives of long chain bases (LCB-DNP) prepared from: (A) a mixture of 3 LCB standards containing t18:0 (phytosphingosine), d18:0 (dihydrosphingosine), and Δ4-d18:1 (sphingosine); (B) wild-type yeast; (C) yeast harboring the *P. nivalis* sphingolipid desaturase expression vector pMON67066; (D) yeast harboring the *P. auricula* sphingolipid desaturase expression vector pMON95048.

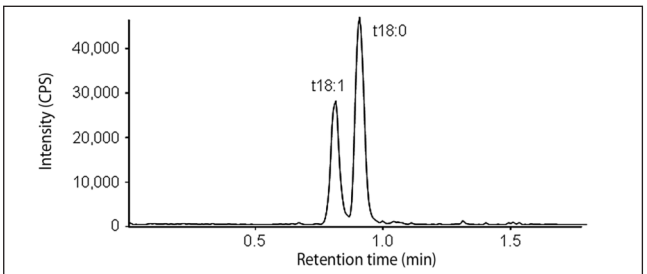

Figure 3. LC–MS–MS analysis of the LCB-DNP derivatives prepared from a yeast sample harboring the *P. nivalis* sphingolipid desaturase expression vector pMON67066. High-throughput HPLC ion chromatogram under MRM mode.

sphingolipids to determine the sphingolipid desaturases activity, they can not identify the actual desaturation site (i.e., the C=C bond position in the mono-unsaturated sphingolipid backbone). A GC–MS method has therefore been designed to solve this problem. As shown in Figure 4, multiple chemical reactions were utilized to convert LCB-DNP derivatives into fatty acid picolinyl compounds, which can be readily detected by GC–MS to locate the C=C position. Briefly, LCB-DNP compound was first oxidized by lead (IV) tetra-acetate into long chain fatty aldehydes by breaking the C-C bond at the diol position (or between –OH and amine carbons for di-hydroxyl bases). Long chain fatty aldehydes can be further oxidized into free fatty acids through a silver reaction (43). The silver reaction is strong enough to oxidize the aldehydes into acids but also gentle enough to leave the C=C bonds intact. The free fatty acids can be readily converted into fatty acid methyl esters (FAME) and eventually fatty acid picolinyl derivatives for GC–MS analysis (44).

Fatty acid picolinyl esters are well-known to be good derivatives available for identification of fatty acyl C=C position by GC–MS (45). They are thermally stable and easy to be separated by GC with polar stationary phases. But most importantly, their electron impact (EI) mass spectra are structural highly informative containing prominent characteristic pyridine ring McLafferty ions at *m/z* = 92, 108, 151, and 164, and easily distinguished molecular ions as always odd-numbered, as well as a series of fragment ions with 14 amu apart for loss of successive methylene groups from the fatty acyl chain. When there is a C=C bond presented in the fatty acyl chain, a distinctive gap of 40 amu at the adjacent methylene group on the carboxyl side, and a clear diagnostic doublet of abundant ions 14 amu apart, representing cleavage on the distal side of the double bond will show up. Putting all of these characters together, one can readily identify the fatty acid esters molecular structure and the C=C bond position in the fatty acyl chain.

For example, shown in Figure 5A is the combined selected ion chromatogram of a LCB standard mixture containing t18:0, Δ4-d18:1, and d18:0. After the previously mentioned wet chemistry reactions, these LCB compounds were transformed into three fatty acids respectively as C15:0, Δ2-C16:1, and C16:0 with an internal standard of fatty acid C17:0. It should be noted here that the lead (IV) tetra-acetate oxidation reaction caused the C-C cleavage in different positions for di-hydroxyl bases and tri-hydroxyl bases, resulting in either loss of two carbons from di-hydroxyl bases or three carbons from tri-hydroxyl bases. In other words, the final product for dehydrophytosphingosine t18:1 is C15:1-fatty acid by losing three carbons but becomes C16:1-fatty acid for di-hydroxyl sphingosine d18:1 LCB by losing only two carbons. Figure 5B and 5C show the mass spectra of Δ2-C16:1 and C15:0-picolinyl derivatives, which are consistent with the spectra reported previously with characteristic pyridine ring rearrangement ions, odd-numbered molecular ions, as well as the characteristic series of fragment ions with 14 amu apart for loss of successive methylene groups (42). Particularly Figure 5B showed the unique diagnostic doublet of abundant ions at *m/z* 177 and 190, indicating the Δ2 C=C position. These results confirm the effectiveness of the wet chemistry assay.

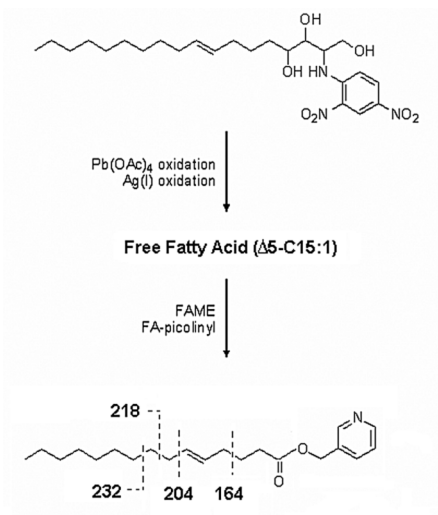

Figure 4. Two-step chemical conversion of Δ8-t18:1-DNP derivative into Δ5-C15:1 free fatty acid by lead (IV) and silver oxidations and then by trans-esterification into fatty acid methyl esters and eventually converted into fatty acid picolinyl esters for GC–MS analysis.

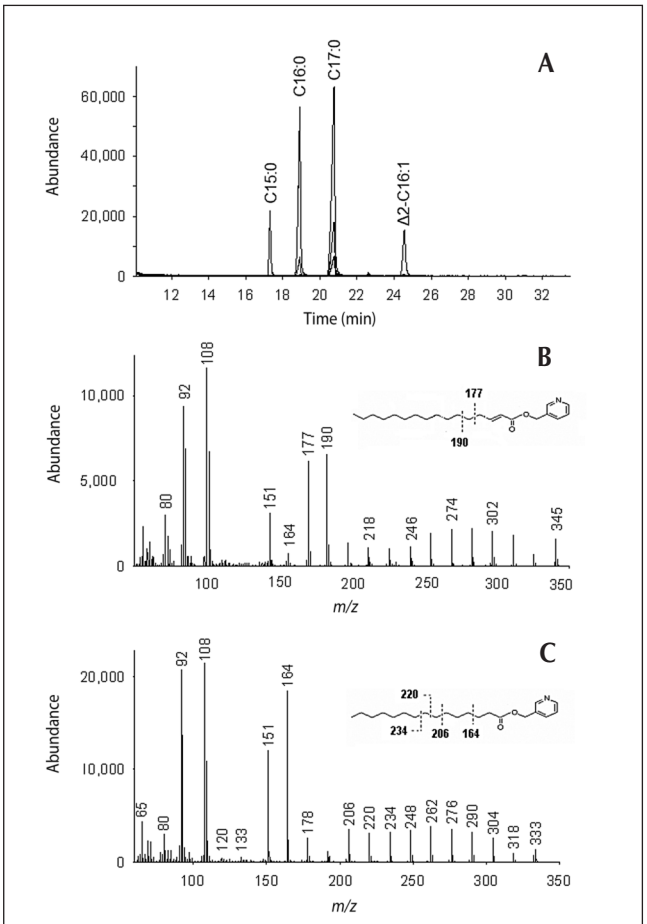

Figure 5. GC–MS analysis of fatty acid picolinyl esters prepared from a mixture of LCB standards containing t18:0 (phytosphingosine), d18:0 (dihydrosphingosine), Δ4-d18:1 (sphingosine), and internal standard C17:0 fatty acid: (A) Combined selected ion chromatograms; (B) EI-mass spectrum of Δ2-C16:1-fatty acyl picolinyl ester as the reaction product of Δ4-d18:1-LCB standard; (C) EI-mass spectrum of C15:0-fatty acyl picolinyl ester as the reaction product of t18:0-LCB standard.

The previous three yeast samples were processed as described in the methods part and analyzed by GC–MS. Figure 6 shows the resultant chromatograms. As in the HPLC chromatogram, the wild-type yeast sample contained only C15:0-fatty acid derived from saturated LCB t18:0. Both sphingolipid desaturase expressing yeast samples contain C15:1-fatty acids with similar cis/trans ratios as to those observed in HPLC analysis. The desaturation position of C15:1 in the fatty acid can be readily located by studying the characteristic diagnostic molecular and fragment ions or comparing to a previous published spectrum. For example, Figure 7 shows the mass spectrum of the C15:1-fatty acid picolinyl derivative of the *P. nivalis* sphingolipid desaturase expressing yeast sample from plasmid pMON67066. Besides the pyridine rearrangement ions at *m/z* 151 and 164 amu, the molecular ion at *m/z* 331 amu reveals the molecular structure as a C15:1 picolinyl ester. Although the gap of 26 amu for the double bond is not easy to locate, that of 40 amu between *m/z* 164–204 serves instead. Only the second ion of the doublet ions at *m/z* 232 stands out, which is a diagnostic ion for Δ5 straight chain monoenoic fatty acid picolinyl ester (45). This result indicates that the corresponding fatty acid precursor is a Δ8-dehydrophytosphingosine, t18:1, and the desaturase is a Δ8 sphingolipid desaturase.

In the yeast assay, the *P. auricula* sphingolipid desaturase produced 66.5% trans double bonds and 33.5% cis double bonds, which is consistent with most reports of prior characterized sphingolipid desaturases. However, the *P. nivalis* enzyme produced 93% cis double bonds, and only 7% trans double bonds. The only other known sphingolipid desaturase that produces predominantly cis double bonds was cloned from *Stylosanthes hamata* and produced cis and trans isomers in a ratio of 4:1 in yeast (16a).

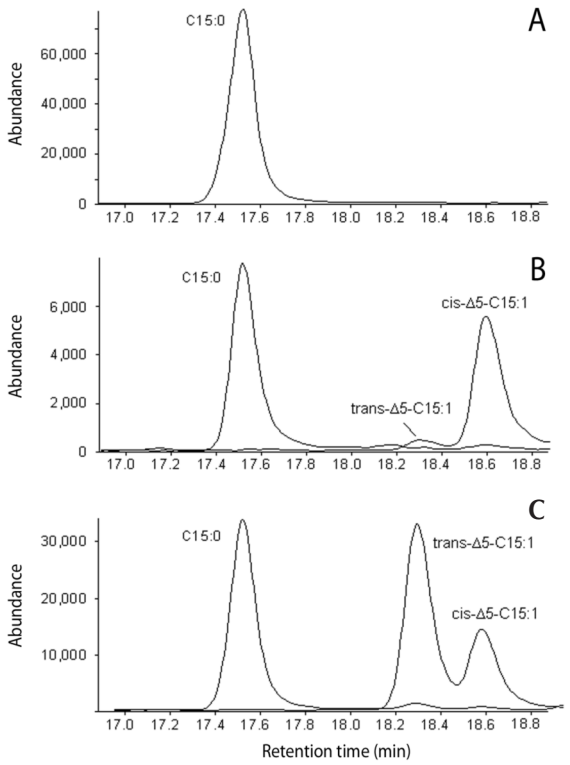

Figure 6. GC–MS selective ion chromatograms of fatty acid picolinyl esters prepared from yeast samples: (A) wild-type yeast; (B) yeast harboring pMON67066; (C) yeast harboring pMON95048.

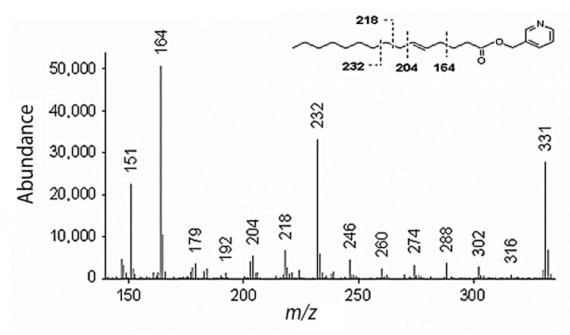

Figure 7. GC–MS EI-mass spectrum of Δ5-C15:1 picolinyl ester prepared from yeast sample harboring the *P. nivalis* sphingolipid desaturase expression vector pMON67066.

Conclusion

In summary, an analytical assay combining reverse phase HPLC–UV, LC–MS–MS, and GC–MS with wet chemistry procedures has been developed to effectively identify the plant sphingolipid desaturase in yeast. Wild-type control and yeast samples expressing sphingolipid desaturase were directly hydrolyzed to convert the sphingolipids into LCB, which could be detected by HPLC–UV or LC–MS–MS as their corresponding DNP (2, 4-dinitrophenyl) derivatives. Mono-unsaturated LCB, dehydrophytosphingosine, t18:1, as the resultant products of sphingolipid desaturase, were detected in transgenic yeast samples with cis, trans-isomers baseline resolution and their structures were confirmed by negative-ion electrospray MS–MS. A high throughput LC–MS–MS method under MRM mode was also developed in order to provide rapid screening of plant sphingolipid desaturases activities. The C=C bond positions of the LCBs were further located by chemical conversion into fatty acid picolinyl derivatives and analyzed by GC–MS to identify the stereo specificity of the sphingolipid desaturase. This assay uses gentle chemicals and reactions that can be easily adapted in industrial and academic laboratories. The use of fatty acid picolinyl derivatives has improved the identification confidence with well-established standard spectra available for comparison. Depending on specific analytical needs, this assay can be employed as either a high throughput screening tool for the rapid selection of active sphingolipid desaturases or as a complete set for the identification for unknown sphingolipid desaturase.

Acknowledgement

The authors thank Monsanto Corp Analytics Pradip Das, Ron Smith, Rochelle Riley, and Jeff Haas at Calgene Campus for their support of this work. Also, the authors thank Keith

Cromack and Pradip Das at Monsanto's Creve Coeur Campus, as well as Jeff Haas, Dan Ovadya, and Adele Contreras at Monsanto's Calgene Campus for their support of this work.

References

1. Y.A. Hannun and L.M. Obeid. Principles of Bioactive Lipid Signaling: Lessons from Sphingolipids. *Nature Rev. Molecular Cell Bio.* **9:** 139–150 (2008).
2. R.C. Dickson. Thematic Review Series: Sphingolipids. New Insights into Sphingolipid Metabolism and Function in Budding Yeast. *J. Lipid Res.* **49:** 909–921 (2008).
3. S.T. Pruett, A. Bushnev, K. Hagedorn, M. Adiga, C.A. Haynes, M.C. Sullards, D.C. Liotta, and A.H. Jr. Merrill. Thematic Review Series: Sphingolipids. Biodiversity of Sphingoid Bases ("Sphingosines") and Related Amino Alcohols. *J. Lipid Res.* **49:** 1621–1639 (2008).
4. H. Jr. Merrill, M.D. Wang, M. Park, and M.C. Sullards. (Glyco)sphingolipidology: An Amazing Challenge and Opportunity for Systems Biology. *Trends in Biochem. Sci.* **10:** 457–468 (2007).
5. M. Chen, G. Han, C.R. Dietrich, T.M. Dunn, and E.B. Cahoon. The Essential Nature of Sphingolipids in Plants as Revealed by the Functional Identification and Characterization of the Arabidopsis LCB1 Subunit of Serine Palmitoyltransferase. *Plant Cell.* **18:** 3576–3593 (2006).
6. M. Chen, J.E. Markham, C.R. Dietrich, J.G. Jaworski, and E.B. Cahoon. Sphingolipid Long-Chain Base Hydroxylation Is Important for Growth and Regulation of Sphingolipid Content and Composition in Arabidopsis. *Plant Cell* **20:** 1862–1878 (2008).
7. V. Ramamoorthy, E.B. Cahoon, M. Thokala, J. Kaur, J. Li, and D.M. Shah. Sphingolipid C9-Methyltransferases Are Important for Growth and Virulence but not for Sensitivity to Antifungal Plant Defensins in Fusarium graminearum. *Eukaryotic Cell* **8:** 217–229 (2009).
8. G.D'Angelo, E. Polishchuk, G. Di Tullio, M. Santoro, A. Di Campli, A. Godi, G. West, J. Bielawski, C.C. Chuang, A.C. van der Spoel, F.M. Platt, Y.A. Hannun, R. Polishchuk, P. Mattjus, and M.A. De Matteis. Glycosphingolipid Synthesis Requires FAPP2 Transfer of Glucosylceramide. *Nature* **449:** 62–67 (2007).
9. K. Sims, S. Spassieva, E. Voit, and L. Obeid Yeast Sphingolipid Metabolism: Clues and Connections. *Biochem. Cell Biol.* **82:** 45–61 (2004).
10. R.P. Rao, C. Yuan, J.C. Allegood, S.S. Rawat, M.B. Edwards, X. Wang, A.H. Jr. Merrill, U. Acharya, and J.K. Acharya. Ceramide Transfer Protein Function is Essential for Normal Oxidative Stress Response and Lifespan. *Proc. Nat. Acad. Sci. USA* **104:** 11364–11369 (2007).
11. W.L. Holland and S.A. Summers. Sphingolipids, Insulin Resistance, and Metabolic Disease: New Insights from in vivo Manipulation of Sphingolipid Metabolism. *Endocrine Rev.* **29:** 381–402 (2008).
12. E. Alewijnse and S.L. Peters. Sphingolipid Signaling in the Cardiovascular System: Good, Bad or Both? *Eur. J. Pharm.* **585:** 292–302 (2008).
13. L.D. Williams, A.E. Glenn, A.M. Zimeri, C. W. Bacon, M.A. Smith, and R.T. Riley. Fumonisin Disruption of Ceramide Biosynthesis in Maize Roots and the Effects on Plant Development and Fusarium Verticillioides-induced Seedling Disease. *J. Agr. Food Chem.* **55:** 2937-2946 (2007).
14. P. Sperling, S. Franke, S. Lüthje, and E. Heinz. Are Glucocerebrosides the Predominant Sphingolipids in Plant Plasma Membranes? *Plant Phys. Biochem.* **42(12):** 1–7 (2005).
15. G. Jenkins, A. Richards, T. Wahl, G. Mao, L. Obeid, and Y. Hannun. Involvement of Yeast Sphinogolipids in the Heat Stress Response of Saccharomyces cervisiae. *J. Bio. Chem.* **272:** 32,566-32,572 (1997).
16. P.R. Ryan, Q. Liu, P. Sperling, B. Dong, S. Franke, and E. Delhaize. A Higher Plant Delta-8 Sphingolipid Desaturase with a Preference for (Z)-isomer Formation Confers Aluminum Tolerance to Yeast and Plants. *Plant Physiol.* **144:** 1968–1977 (2007).
17. H. Jr. Merrill, M.C. Sullards, J.C. Allegood, S. Kelly, and E. Wang. Sphingolipidomics: High-throughput, Structure-specific, and Quantitative Analysis of Sphingolipids by LC–MS–MS. *Methods* **36:** 207–224 (2005).
18. M.C. Sullards, J.C. Allegood, S. Kelly, E. Wang, C.A. Haynes, H. Park, Y. Chen Y, and A.H. Jr Merrill. Structure-specific, Quantitative Methods for Analysis of Sphingolipids by Liquid Chromatography-Tandem Mass Spectrometry: "Inside-out" Sphingolipidomics. *Methods Enzym.* **432:** 83–115 (2007).
19. L.A. Cowart and Y.A. Hannun. Using Genomic and Lipiomic Strategies to Investigate Sphingolipid Function in the Yeast Heat-Stress Response. *Biochem. Soc. Transactions* **33:** 1166–1169 (2005).
20. Y. Chen, J. Allegood, Y. Liu, E. Wang, B. Cachón-Gonzalez, T.M. Cox, A.H. Jr Merrill, and M.C. Sullards. Imaging MALDI Mass Spectrometry Using an Oscillating Capillary Nebulizer Matrix Coating System and its Application to Analysis of Lipids in Brain from a Mouse Model of Tay-Sachs/Sandhoff Disease. *Anal. Chem.* **80:** 2780–2788 (2008).
21. P. Sperling, and E. Heinz. Plant Sphingolipids: Structural Diversity, Biosynthesis, First Genes and Functions. *Biochimica et Biophysica Acta* **1632:** 1–15 (2003).
22. J.E. Markham, J. Li, E.B. Cahoon, and J.G. Jaworski. Plant Sphingolipids: Separation and Identification of Major sphingolipid classes from leaves. *J. Biol. Chem.* **281:** 22,684–22,694 (2006).
23. R.L. Lester and R.C. Dickson. High-Performance Liquid Chromatography Analysis of Molecular Species of Sphingolipid-Related Long Chain Bases and Long Chain Base Phosphates in Saccharomyces cerevisiae after Derivatization with 6-Aminoquinolyl-N-hydroxysuccinimidyl Carbamate. *Anal. Biochem.* **298:** 283–292 (2001).
24. P. Sperling, A. Blume, U. Zähringer, and E. Heinz. Further Characterization of Δ8-Sphingolipid Desaturases from Higher Plants. *Biochem. Soc. Transactions* **28:** 638–641 (2000).
25. C. Beckmann, J. Rattke, N.J. Oldhan, P. Sperling, E. Heinz, and W. Boland. Characterization of a Δ8-Sphingolipid Desaturase From Higher Plants: A Stereochemical and Mechanistic Study on the Origin of E,Z Isomers. *Angew. Chem. Int. Ed.* **41:** 2298–2300 (2002).
26. P. Sperling, B. Libisch, U. Zähringer, J.A. Napier, and E. Heinz. Functional Identification of a Δ8-sphingolipid Desaturase from Borago officinalis. *Arch. Biochem. Biophys.* **388:** 293–298 (2001).
27. P. Ternes, S. Franke, U. Zähringer, P. Sperling, and E. Heinz. Identification and Characterization of a Sphingolipid Δ4-Desaturase Family. *J. Bio. Chem.* **277:** 25,512–25,518 (2002).
28. P. Sperling, U. Zähringer, and E. Heinz. A Sphingolipid Desaturase from Higher Plants. *J. Bio. Chem.* **273:** 28,590–28,596 (1998).
29. V. Sayanova, F. Beaudoin, L.V. Michaelson, P.R. Shewry, and J. Napier. Identification of Primula Fatty Acid Delta 6-desaturases with n-3 Substrate Preferences. *FEBS Lett.* **542:** 100–104 (2003).
30. F. García-Maroto, J.A. Garrido-Cárdenas, J. Rodríguez-Ruiz, M. Vilches-Ferrón, A.C. Adam, J. Polaina, and D.L. Alonso. Cloning and Molecular Characterization of the Δ6-desaturase from two Echium plant species: production of GLA by heterologous expression in yeast and tobacco. *Lipids* **37:** 417–426 (2002).
31. H. Ochman, M.M. Medhora, D. Garza, and D.L. Hartl. Amplification of Flanking Sequences by Inverse PCR. In M.A. Innis, D.H. Geldfand, J. J. Sninsky, T.J. White, PCR Protocols: A Guide to Methods and Applications, Academic Press, San Diego, 1990, pp. 219–227.
32. J. Sambrook, and D. Russell. Molecular Cloning: A Laboratory Manual, Cold Spring Harbor Laboratory Press, Cold Spring Harbor, New York, 2001.
33. O. Sayanova, M.A. Smith, P. Lapinskas, A. K. Stobart, G. Dobson, W.W. Christie, P.R. Shewry, and J. A. Napier. Expression of a Borage Desaturase cDNA Containing an N-terminal Cytochrome b5 Domain Results in the Accumulation of High Levels of Δ6-desaturated Fatty Acids in Transgenic Tobacco. *Proc. Natl. Acad. Sci. USA* **94:** 4211–4216 (1997).
34. J. Shanklin, E. Whittle, and B.G. Fox. Eight Histidine Residues Are Catalytically Essential in a Membrane-associated Iron Enzyme, Stearoyl-CoA Desaturase, and Are Conserved in Alkane Hydroxylase and Xylene Monooxygenase. *Biochem.* **33:** 12787–12794 (1994).
35. W. Griffiths, A. Jonsson, S. Liu, D. Rai, and Y. Wang. Electrospray and Tandem Mass Spectrometry in Biochemistry. *Biochem. Soc.* **355:** 545–561 (2001).
36. B. Lieser, G. Liebisch, W. Drobnik, and G. Schmitz. Quantification of Sphingosine and Sphingasine from Crude Lipid Extracts by HPLC Electrospray Ionization Tandem Mass Spectrometry. *J. Lipid Res.* **44:** 2209–2216 (2003).
37. J.E. Markham and J.G. Jaworski. Rapid Measurement of Sphingolipids from Arabidopsis thaliana by Reversed-phase High-performance Liquid Chromatography Coupled to Electrospray Ionization Tandem Mass Spectrometry. *Rapid Comm. Mass Spec.* **21:** 1304–1314 (2006).
38. F. Hsu, J. Turk, M. Stewart, and D. Downing. Structural Studies on Ceramides as Lithiated Adducts by Low Energy Collisional-Activated Dissociation Tandem Mass Spectrometry with Electrospray Ionization. *Am. Soc. Mass Spec.* **13:** 680–695 (2002).
39. M. Gu, J. Kerwin, J. Watts, and R. Aebersold. Ceramide Profiling of Complex Lipid Mixtures by Electrospray Ionization Mass Spectrometry. *Anal. Biochem.* **244:** 347–356 (1997).
40. N. Mano, Y. Oda, K. Yamad, N. Asakawa, and K. Katayama. Simultaneous Quantitative Determination Method for Sphingolipid Metabolites by Liquid Chromatography/Ionspray Ionization Tandem Mass Spectrometry. *Anal. Biochem.* **244:** 291–300 (1997).
41. E. Berdyshev, I. Gorshkova, J. Garcia, V. Natarajan, and W. Hubbard. Quantitative Analysis of Sphingoid Base-1-Phosphates as Bisacetylated Derivatives by Liquid Chromatography-Tandem Mass Spectrometry. *Anal. Biochem.* **339:** 129–136 (2005).
42. W. Seefelder, G. Schwerdt, R. Freudinger, M. Gekle, and H.-U. Humpf. Liquid Chromatography/Electrospray Ionization-Mass Spectrometry Method for the Quantification of Sphingosine and Sphinganine in cell cultures exposed to Fumonisins. J. Chromatogr. B 780: 137–144 (2002).
43. P. Ferraboschi, R. Canevotti, P. Grisenti, and E. Santaniello. A New Flexible Synthesis of (R,S)-Mevalonolactone. *J. Chem. Soc. Perkin Trans.* 2301–2303 (1987).
44. F. Destaillats and P. Angers. One-Step Methodology for the Synthesis of FA Picolinyl Esters from Intact Lipids. *J. Am. Oil Chem. Soc.* **79:** 253–256 (2002).
45. W.W. Christie, E.Y. Brechany, and R.T. Holman. Mass Spectra of the Picolinyl Esters of Isomeric Mono- and Dienoic Fatty Acids. *Lipids* **22:** 224–228 (1987).

Manuscript received December 2, 2008;
Revision received March 8, 2008.